TRANSACTIONS OF THE INSTITUTE OF FLUID-FLOW MACHINERY

No. 131, 2016, 161–172

Eliza Tkacz*, Zbigniew Kozanecki, Jakub Łagodziński

Hybrid bearing development for high-speed turbomachinery in distributed energy systems

Institute of Turbomachinery, Lodz University of Technology,
219/223 Wólczańska, 90-924 Łódź, Poland

Abstract

In the paper authors undertake the design of hydrostatic bearings and hybrid bearings for a specific application – hermetic high–speed turbogenerators for the electric power generation. The most common hydrostatic bearings are usually oil lubricated. On the contrary, the considered here machines are dedicated for the combined heat and power (CHP) production in organic Rankine cycle (ORC) systems and so the hydrostatic bearings use an organic, oil-free working fluid as the lubricant. The reader will acquire an insight into the special characteristics of hydrostatic bearings. Moreover, a new type of bearings, a hybrid bearing, is introduced, which combine both, hydrostatic and hydrodynamic effects. The designed bearings have been manufactured and their good performance confirmed during tests on a real machine.

Keywords: Oil-free bearings; Organic Rankine cycle turbomachinery; Design and manufacturing

1 High-speed turbomachinery in distributed energy systems

In distributed power generation dedicated to combine heat and power systems (CHP), microturbines of a power output ranging between 1 and 100 kW and rotational speeds of approximately 15000–40000 are applied. A small power system can be based on the organic Rankine cycle (ORC) with a low boiling working medium, [1]. The existing conventional oil-lubricated bearings reveal performance

*Corresponding Author. Email address: eliza.tkacz@p.lodz.pl

limits at high revolutions, especially when stability of the bearing is taken into account. Furthermore, in order to maintain the purity of the cycle, we are searching for hermetic machines equipped with bearings lubricated with the working medium.

For microturbines of electrical power output of about 1–3 kW, special gas bearings can be used [2,3]. Here, the electrical power output of the turbogenerator is up to 80 kW and for the machine of such size and loading gas bearings reach performance limits. The bearing system needs to be liquid lubricated and the hermetic construction of the machine is shown in Fig. 1. The turbine working medium is an organic fluid, the siloksan MDM, the properties of which are listed in Tab. 1. Main parameters of the machine are presented in Tab. 2. The designed machine is the turbogenerator with a one stage supersonic flow impulse turbine and dedicated measurement and control system. For monitoring and diagnostics the reader can consult [4, 5].

Table 1: MDM properties.

Temperature, °C	60	80	90
Density, kg/m^3	780.86	759.68	749.09
Viscosity, Pa s	5.24×10^{-4}	4.465×10^{-4}	4.072×10^{-4}

Table 2: Main parameters of the designed turbogenerator.

Parameter	Value
Inlet pressure at inlet temperature, $T_{\text{in}} = 248\,^{\circ}\text{C}$, P_{in}	0.7 MPa
Outlet pressure, P_{out}	0.017 MPa
Flow rate, $\dot{m}$	1.57 kg/s
Rotational speed	20000 rpm
Maximum electrical power output	80 kW
Bearing system	hermetic, oil free

Liquid lubricated bearings are widely described in the literature in therms of design and performance [6, 7] or numerical simulations and performance [8]. In this paper, the dedicated hybrid bearings design is described, which meet the requirements of low friction, low wear and high accuracy. Two designed bearings are not equally loaded and so the drive end (DE or turbine side) bearing and the non

drive end (NDE) bearing are distinguished. Good bearing system performance was confirmed during turbogenerator tests.

2 Hybrid bearings design

In hybrid bearings both hydrostatic and hydrodynamic effects are used. Hydrostatic bearings employ a liquid pressurized lubricant [6]. Lubricant at a constant supply pressure, P_s, is pumped towards the bearing and it first passes through a flow control device – the restrictor (Fig. 2). The dissipation of pressure energy causes pressure reduction on entry into the recess of the bearing pad. Pressure in the recess, P_r, is assumed to remain constant throughout the recess volume. The flow then leaves through the thin clearance between the bearing land and the journal surface. The pressure reduction across the land is observed and it reaches ambient pressure at the outside edge.

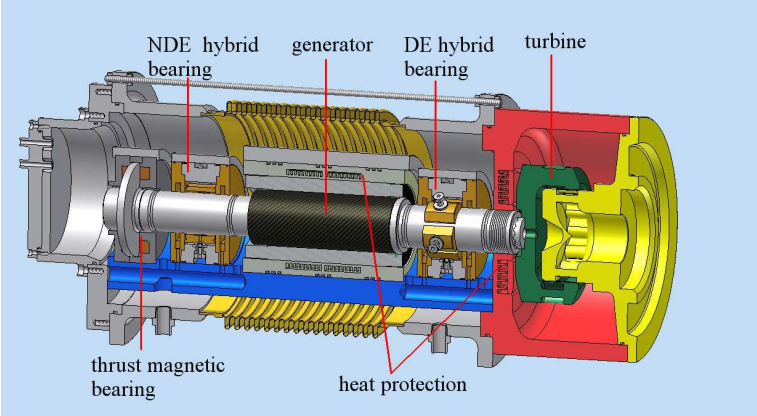

Figure 1: 3D model of the designed turbogenerator with its bearing system.

The great advantage of hydrostatic bearings is the complete separation of the solid sliding surfaces with a fluid film. Because the pressurized film is not produced by the relative motion of the bearing surfaces, a complete film is present whenever the bearing is pressurized, even at zero speed. An essential feature of an externally pressurized bearing is a compensation mechanism, the purpose of which is to allow the pressure in the recess to be adjusted in response to an external load. In Fig. 2 four recesses are supplied with a liquid lubricant, each through a separate restrictor. The dissipation of energy in the restrictor causes the recess pressure to be lower than the supply pressure: $P_1 < P_s$, $P_2 < P_s$, $P_3 < P_s$, and $P_4 < P_s$.

When an external load is applied to the shaft, the thin clearance is reduced in the direction of the applied load. The pressure in the corresponding recess is now higher than in the opposite one. This mechanism is more simple to understand if the reader imagines an extreme case, when a very high applied load would force the bearing surfaces together and prevent the side flow. The pressure in the recess would rise until it would equal the supply pressure. From this example, one can expected the pressure rise, when the clearance is reduced and similarly – the pressure drop, when the clearance increases.

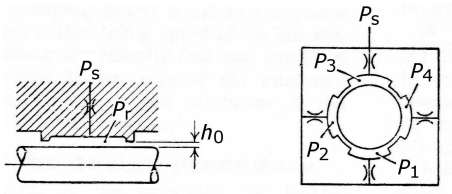

Figure 2: Diagrammatic representation of a typical hydrostatic journal bearing, h_0 denotes a radial clearance.

In order to calculate the magnitude of the applied load which can be supported, it is necessary to establish the pressure distribution in the bearing and then to sum the product of pressure times area over the bearing surface. For a specify extreme load, W', there must be a certain pressure in the recess equal to:

$$P_{\mathrm{r}} = \frac{W'}{A_{\mathrm{r}}} \,, \tag{1}$$

where A_{r} is a recess area. Then, the supply pressure is $P_{\mathrm{s}} = \beta P_{\mathrm{r}}$, with $\beta = 0.5$. However, the designer will usually provide for at least a 20% excess of pump capacity, to allow for manufacturing tolerances and variations on temperature. In order to decide value of P_{s} to be used, the minimum value can be estimated from the relation

$$P_{\mathrm{s}}(\min) = \frac{3W'}{\bar{\lambda}_0 D(L-a)} \,, \tag{2}$$

where D is the bearing diameter, L – bearing length, a – width of axial flow land and $\bar{\lambda}_0$ – dimensionless stiffness for journal bearings with n pads, axial slots and capillary restrictors.

Calculated parameters of hydrostatic bearings used for the project needs are presented in Tabs. 3 and 4.

The hydrodynamic bearing is said ‘self–acting’ because the hydrodynamic pressures which separate the two bearing surfaces are generated as a consequence

Table 3: Static parameters of the non drive end (NDE) hybrid bearing.

Parameter	Value	Unit
static load, $W_{\max}$	32	N
lubricant temperature at inlet, T_z	70	°C
dynamic viscosity, η	4.85×10^{-4}	Pa s
number of pads	5	–
bearing length, L	50	mm
bearing diameter, D	58	mm
radial clearance, C	0.051	mm
eccentricity, e	0.094	–
minimum supply pressure, P_s	1.52×10^5	Pa
designed recess pressure, P_r	0.75×10^5	Pa
dynamic stiffness, $K_{XX} \approx K_{YY}$	6.7×10^6	N/m
total flow rate, q_0	4.84	l/min

Table 4: Static parameters of the drive end (DE) hybrid bearing.

Parameter	Value	Unit
static load, $W_{\max}$	277	N
lubricant temperature at inlet, T_z	70	°C
dynamic viscosity, η	4.85×10^{-4}	Pa s
number of pads	5	–
bearing length, L	50	mm
bearing diameter, D	70	mm
radial clearance, C	0.052	mm
eccentricity, e	0.190	–
minimum supply pressure, P_s	4.83×10^5	Pa
designed recess pressure, P_r	2.4×10^5	Pa
dynamic stiffness, $K_{XX} \approx K_{YY}$	2.35×10^7	N/m
total flow rate, q_0	13.12	l/min

of the movement of the bearing surfaces. The moving element drags liquid by means of the viscous forces into the converging gap region. The result of the liquid being dragged into a more confined region is to create a back pressure. This build-up of pressure produces a bearing film force separating the two solid surfaces. The resultant of the hydrodynamic forces acts normally to the shaft and

it is opposite to the externally applied force on the shaft. For a given eccentricity of the journal, e, the pressure force is primarily dependent on speed, ω, viscosity, η, and bearing area. If the speed in a hydrodynamic journal bearing is zero, there is no bearing film force. For this reason, starting and stopping are the major causes of wear in correctly designed hydrodynamic bearings. This problem does not arise in hydrostatic bearing where the external pressure is switched on before start-up.

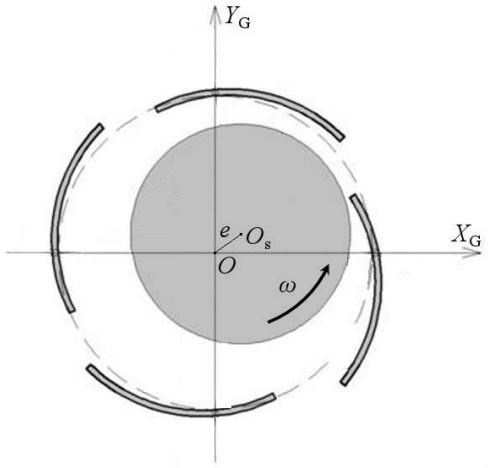

Figure 3: Diagrammatic representation of a tilting pad bearing, O_s denotes the journal center and Y_GOX_G – global coordinate system.

There are different types of hydrodynamic bearings and one of them is a tilting pad bearing. A significant aspect of this solution is a presence of movable non-rotating elements – tilting pads (Fig. 3). The motion of tilting pads generates friction forces in the tilting shoe support and, thus, it can affect dramatically dynamic characteristics of the bearing. Therefore, the calculation of dynamic properties of tilting pad bearings may be troublesome. According to the linear theory, for a constant rotational speed and a static force, these properties are usually represented by a set of eight coupled dynamic coefficients, linearised around the static equilibrium position. This simplification is possible on an assumption of small displacements of the shaft center in the closest vicinity of the equilibrium position. It is necessary to limit the scale of the excitation forces in order to fulfill the basic condition of small displacements.

For the project needs two tilting pads bearings have been designed. The pressure distribution in the bearing clearance and bearing properties are presented in Figs. 4 and 5, where $\mathbf{K}$ denotes the matrix of stiffness coefficients and $\mathbf{B}$ – damping coefficients.

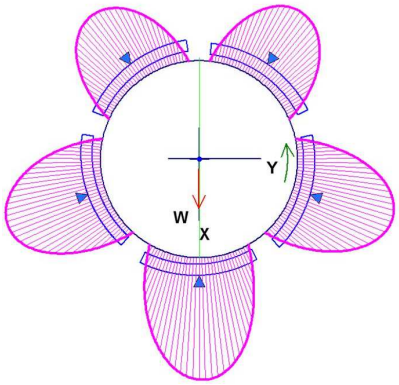

$\frac{L}{D} = 0.8621$, $C = 0.052$ mm, $\frac{e}{C} = 0.0819$
$\omega = 20000$ rpm, $W = 32$ N
$\eta = 4.661 \times 10^{-4}$ Pa s
$T = 70.0, 70.6, 71.1$ °C
$P_{\max} = 105.9$ kPa
$\dot{Q}_{\text{sup}} = 15$ l/min, $\dot{Q}_{\text{side}} = 3.251$ l/min

$$\mathbf{K} = \begin{vmatrix} 5.171 \times 10^3 & 0 \\ 0 & 5.325 \times 10^3 \end{vmatrix} \text{ [N/mm]}$$

$$\mathbf{B} = \begin{vmatrix} 3.280 & 0 \\ 0 & 3.330 \end{vmatrix} \text{ [Ns/mm]}$$

Figure 4: Pressure distribution and hydrodynamic parameters calculated for the non drive end (NDE) hybrid bearing.

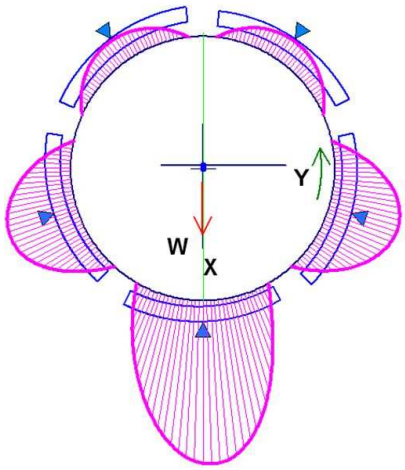

$\frac{L}{D} = 0.7143$, $C = 0.052$ mm, $\frac{e}{C} = 0.3515$
$\omega = 20000$ rpm, $W = 277$ N
$\eta = 4.647 \times 10^{-4}$ Pa · s
$T = 70.0, 71.0, 72.4$ °C
$P_{\max} = 353.4$ kPa
$\dot{Q}_{\text{sup}} = 15$ l/min, $\dot{Q}_{\text{side}} = 4.730$ l/min

$$\mathbf{K} = \begin{vmatrix} 1.001 \times 10^4 & 0 \\ 0 & 1.777 \times 10^4 \end{vmatrix} \text{ [N/mm]}$$

$$\mathbf{B} = \begin{vmatrix} 5.716 & 0 \\ 0 & 7.925 \end{vmatrix} \text{ [Ns/mm]}$$

Figure 5: Pressure distribution and hydrodynamic parameters calculated for the drive end (DE) hybrid bearing.

Based on previously described calculations, hybrid bearings were designed to take maximum advantage of hydrostatic and hydrodynamic effects. Hybrid bearings are actually five tilting pads bearings with supply orifices in each pad. The bearing 3D model is presented in Fig. 6 and for its technical drawing see Fig. 7. The design offers start-ups without any wear, good bearing film stiffness at zero speed and high overload capacity when operating at full speed.

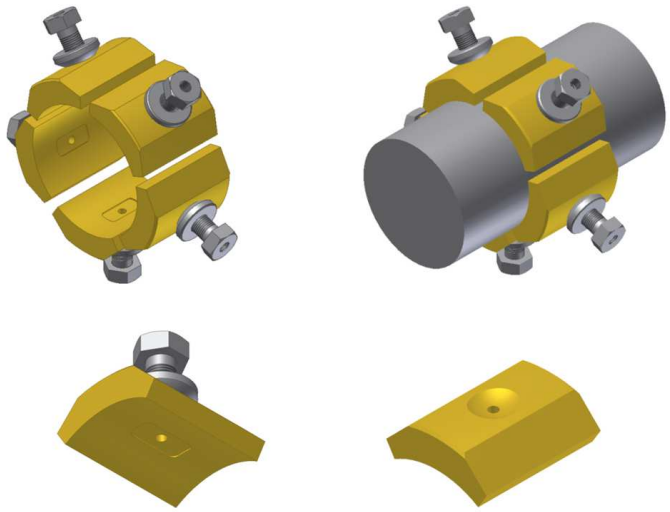

Figure 6: 3D model of the bearing construction.

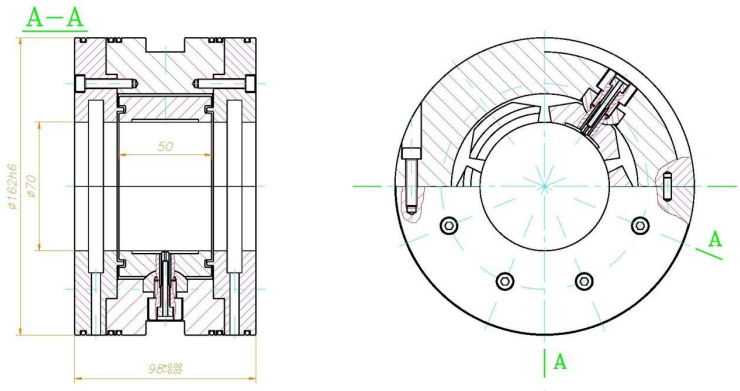

Figure 7: Technical drawing of a hybrid bearing.

For the bearing supply, the integral MDM circuit has been built (see Fig. 8). It is equipped with a gear pump with its electric motor, electric inverter, the supply pressure control and safety system. At the bottom of the turbogenerator housing, outflow orifices have been designed, through which the side flow lubricant is gravitationally evacuated. A special labyrinth seal supplied with a cooler is used at the turbine side for heat protection of bearings. In the bearing housing seals and outflow orifices are designed in order to prevent lubricant leakages (Fig. 9b).

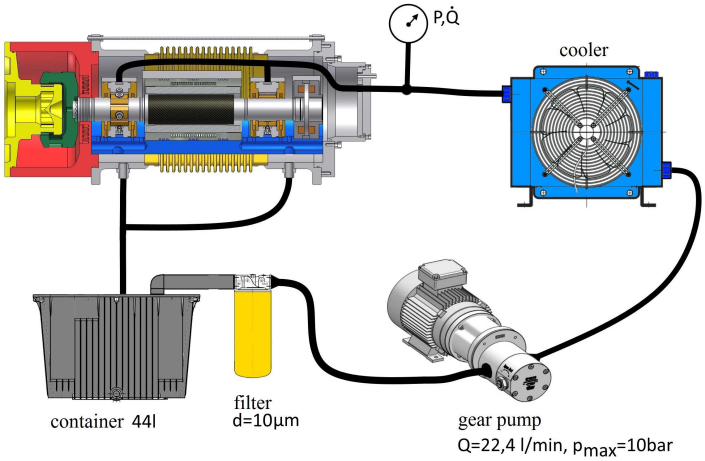

Figure 8: MDM supply system

3 Hybrid bearings tests

As it is well known, the particular role in rotor dynamics is played by bearings. Their dynamic properties, damping and stiffness, decide on vibrations amplitudes and modes of rotating system critical frequencies. For the sake of numerical simulations, the simplification of small displacements of the shaft center in the closest vicinity of the equilibrium position has been made. Otherwise, the nonlinear modeling of dynamic properties of a variable geometry bearing, including design characteristics of the support and generated friction forces, would have to be undertaken. Therefore, in order to confirm the good stability of the rotating system with hybrid bearings, experimental tests have been conducted.

The bearing system was tested in ambient temperature of about 23 °C, when the turbine was driven by compressed air. The machine was tested up to 7260 rpm, so below the first critical speed, while the amplitude of vibrations and phase of vibrations were monitored. The test bench is shown in Fig. 9. First, the photograph of hybrid bearings working surfaces after conducted tests confirms the correct operation of the bearings in given range of loads and rotational speeds. Second, the cascade plots (Figs. 10 and 11) prove the stability of the machine rotating system during the start-up and at the shut-down. At the drive end (DE) the amplitude of vibrations was about 11 μm and on non drive end (NDE) – no greater than 17 μm. Other measurements show that the total volumetric flow of the incoming low viscosity siloxane MDM through a single hybrid bearing is about

8 l/min, when the supply pressure is less than 0.6 MPa. The reader should note, that in previously described theoretical calculations and numerical simulations, hydrostatic effects were dissociated from hydrodynamic effects. That is why, the experimental volumetric flow, where both hydrodynamic and hydrostatic effects are present, differs from the calculated one. Moreover, unlike experimental tests, the calculations were made for the working medium temperature of 70 °C.

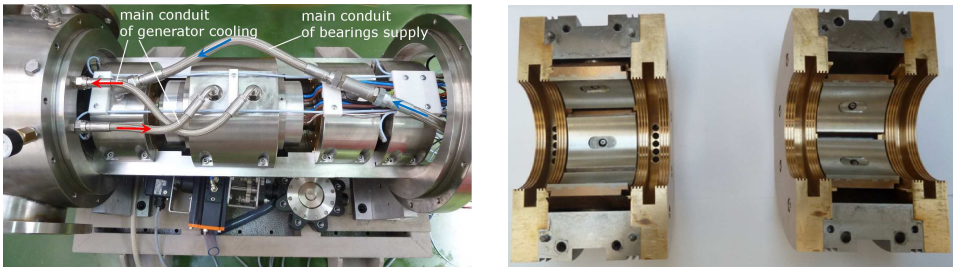

a b

Figure 9: Turbogenerator test bench: a) bearing supply system; b) hybrid bearing surface state after cunducted tests.

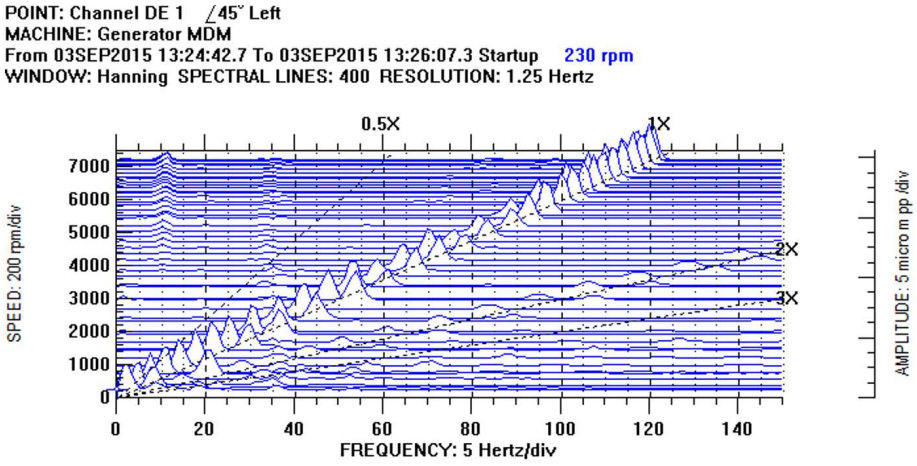

Figure 10: Amplitude of vibration on DE bearing during the start-up of the turbogenerator.

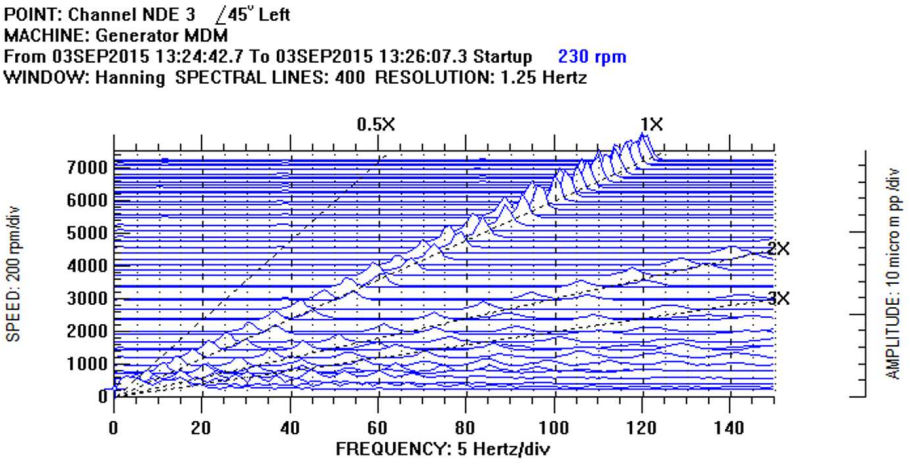

Figure 11: Amplitude of vibration on NDE bearing during the start-up of the turbogenerator.

4 Conclusions

In the study, the rotating system of the ORC turbogenerator equipped with hybrid bearings lubricated with the liquid silixane MDM has been build and tested under ambient temperature. Achieved results allow us to draw the following conclusions and comments:

- The machine was tested up to 7260 rpm in ambient temperature of about 23 °C. The rotational speed was limited by the rate of delivery of compressed air system and not by hybrid bearings performance. More precisely, the bearing system was designed to support the nominal speed of 20 000 rpm.
- Measurements of relative vibration on the bearings as well as other measurements confirm the stable work in the analysed range of speeds and loads. This finding was supported by the ideal condition of working surfaces of bearings after conducted tests.
- The results of the tests are positive, and allow us to choose the design concept as a technical solution for the machine construction and to approve the machine for farther tests on the target installation.

Received in July 2016

References

[1] Kaczmarczyk T.Z., Żywica G., Ihnatowicz E: *The experimental investigation of the biomass-fired orc system with a radial microturbine.* Appl. Mech. Mater. **831**(2016), 235–244.

[2] Kozanecki Z., Tkacz E., Łagodziński J., Miazga K.: *Theoretical and experimental investigations of oil-free bearings and their application in diagnostics of high-speed turbomachinery.* [In :] Smart Diagnostics V, Trans Tech Publ.,**588**, 2014, 302–309.

[3] Kozanecki Z., Tkacz E., Lagodzinski J., Miazga K.: *Oil-free bearings for hermetic high-speed turbomachinery.* J. Vibration Eng. Technol. **2**(2014), 4, 351–360.

[4] Kozanecki Z., Kozanecka D., Klonowicz P., Łagodziński J.,.Gizelska M., Tkacz E., Miazga K., Kaczmarek A.: *Oil-free low power fluid-flow machinery.* Wydawnictwo Instytutu Maszyn Przepływowych PAN, Gdańsk 2014 (in Polish).

[5] Gizelska M.: *Monitoring and diagnostics of special-purpose turbomachines.* Open Eng. **5**(2015), 1, 500–508.

[6] Rowe W.B.: *Chapter 1 – Application.* [In :] Hydrostatic, Aerostatic and Hybrid Bearing Design (W.B. Rowe, Ed.), Oxford: Butterworth-Heinemann 2012, 1–23.

[7] Frêne J., Nicolas D., Degueurce B., Berthe D., Godet M.: *Lubrification hydrodynamique. Paliers et Butées.* Cellection de la Direction des études et recherches d'électricité de France, Eyrolles ed., Paris 1990.

[8] Żywica G., Drewczyński M., Kiciński J., Rządkowski R.: *Computational modal and strength analysis of the steam microturbine with fluid-film bearings.* J. Vib. Eng. Technol. **2**(2014), 6, 543–549.